Liu et al. BMC Complementary and Alternative Medicine (2016) 16:423
DOI 10.1186/s12906-016-1383-7

BMC Complementary and Alternative Medicine

RESEARCH ARTICLE Open Access

Sarcandra glabra (Caoshanhu) protects mesenchymal stem cells from oxidative stress: a bioevaluation and mechanistic chemistry

Jingjing Liu[1], Xican Li[1*], Jian Lin[2], Yunrong Li[1], Tingting Wang[1], Qian Jiang[1] and Dongfeng Chen[2*]

Abstract

Background: *Sarcandra glabra* (Caoshanhu) is a traditional Chinese herbal medicine used for treating various oxidative-stressed diseases. The present work evaluated its protective effect on mesenchymal stem cells (MSCs) from oxidative stress and then discussed possible mechanisms underlying this observation.

Methods: Ethanolic extract of *S. glabra* (ESG) was investigated by chemical methods for its content of total phenolics, rosmarinic acid, and astilbin. ESG, along with rosmarinic acid and astilbin, was investigated for the effect on the viability of Fenton-treated MSCs using 3-(4,5-Dimethylthiazol-2-yl)-2,5-diphenyl (MTT) assay. The observed cell protective effect was further explored by mechanistic chemistry using various antioxidant assays, including DNA protection, •OH-scavenging, $\bullet O_2^-$-scavenging, FRAP (ferric ion reducing antioxidant power), $ABTS^+\bullet$-scavenging, DPPH•-scavenging, and Fe^{2+}-chelating assays.

Results: Analysis of ESG revealed a content of 46.31 ± 0.56 mg quercetin/g total phenolics, 0.78 ± 0.01 % rosmarinic acid, and 3.37 ± 0.01 % astilbin. Results from the MTT assay revealed that three compounds (rosmarinic acid>astilbin>ESG) could effectively increase the survival of Fenton-treated MSCs. Similarly, in $\bullet O_2^-$-scavenging, DPPH•-scavenging, and Fe^{2+}-chelating assays, rosmarinic acid exhibited more activity than astilbin; while in FRAP, $ABTS^+\bullet$-scavenging assays, astilbin was stronger than rosmarinic acid.

Conclusion: *S. glabra* can prevent MSCs from •OH-induced oxidative stress. Such protective effect can be attributed to its antioxidant ability and the presence of two kinds of phytophenols, i.e. caffeoyl derivatives and flavonoids. As the respective representatives of caffeoyl derivatives and flavonoids, rosmarinic acid and astilbin may exert the antioxidant action via direct ROS-scavenging and indirect ROS-scavenging (i.e. Fe^{2+}-chelating). The direct ROS-scavenging ability involves hydrogen atom transfer (HAT) and/or electron transfer (ET) pathway. Astilbin engages the latter pathway more, which can be attributed to the larger planar conjugation in A/C fused rings. Rosmarinic acid, on the other hand, shows more HAT and Fe^{2+}-chelating potential, which may be due to rosmarinic acid bearing one more catechol moiety whereas astilbin has steric-hindrance from 3-α-L-rhamnose and an H-bonding between 4,5 sites. The antioxidant features of rosmarinic acid can be generalized to other caffeoyl derivatives, while that of astilbin cannot be generalized to other flavonoids because of the difference in chemical structures.

Keywords: Antioxidant mechanism, Astilbin, Caoshanhu, Electron transfer, Fe-chelating, Hydrogen atom transfer, Mesenchymal stem cells, Rosmarinic acid, *Sarcandra glabra*

* Correspondence: lixican@126.com; cdf27212@21cn.com
[1]School of Chinese Herbal Medicine, Guangzhou University of Chinese Medicine, Waihuan East Road No.232, Guangzhou Higher Education Mega Center, 510006 Guangzhou, China
[2]School of Basic Medical Science, Guangzhou University of Chinese Medicine, Guangzhou, China, 510006

Background

Owing to the ease of isolation, manipulability, and potential for differentiation, mesenchymal stem cells (MSCs) are of great interest to clinicians for their great potential to enhance tissue engineering for the treatment of various diseases [1], especially neurodegenerative diseases [2], osteoarthritis [3], and cancers [4]. However, during the process of proliferation and differentiation, chemical or physical stimuli, such as radiation [5] and iron overload [6], can generate the •OH radical to cause oxidative stress-induced apoptosis of these cells. This poor viability has prevented the clinical application of the transplantation of MSCs.

In fact, in autologous stem cell transplantation for cancer patients, radiotherapy has been recently indicated to decrease cell survival [7]. The most recent study pointed out that MSCs can even promote tumor recurrence after stereotactic body radiation therapy [8]. These are believed to be related to the oxidative stress induced by reactive oxygen species ROS, especially •OH (the most toxic form of ROS) [9].

Interestingly, traditional Chinese Medicine (TCM) views this oxidative-stressed apoptosis, as well as the dysfunction of viability, proliferation, and differentiation, as a syndrome arising from so-called *heat-toxic*. The *heat-toxic* can be countered by a great deal of Chinese herbal medicines, such as Caoshanhu (or Zhongjiefeng, Fig. 1a).

Caoshanhu is the dried whole plant of *Sarcandra glabra* (Thunb.) Nakai (*S. glabra*, Fig. 1b), which is a shrub widely distributed in China and other Asian countries. In TCM, *S. glabra* is frequently used to treat various diseases relevant to heat-toxic, especially pneumonia, epidemic encephalitis B, appendicitis, shigellosis, and cancers [10]. All of these diseases however have been suggested to be linked to oxidative stress, in free radical biology and medicine [11]. This implies that *S. glabra* will be able to play a role in repairing apoptosis of MSCs in the transplantation process.

Fig. 1 The photos of Caoshanhu (**a**) and the plant of *Sarcandra glabra* (Thunb.) Nakai (**b**)

Phytochemical study has shown that, *S. glabra* contains at least 50 components that can be classified into five types: organic acids, caffeoyl derivatives, flavonoids, coumarins, and terpenoids [12, 13]. Caffeoyl derivatives and flavonoids were newly reported to be the first main bioactive compounds; while isofraxidin (a coumarin) was considered as the second main bioactive compound [14]. As such, rosmarinic acid (RA) and astilbin (AS) were selected as the two typical bioactive compounds in the present study. It is worth noting that isofraxidin is utilized as the "marker compound" in Zhongjiefeng Tablet in *Chinese Pharmacopoeia* [10]. However, isofraxidin is actually less relevant to the present study.

Consequently, in present study we comparatively investigated the effects of *S. glabra*, RA, and AS toward the viability of oxidative-stressed MSCs, then further discussed the possible mechanistic chemistry based on the structure-activity relationship of RA and AS. This approach will help understand the beneficial effects of *S. glabra* as a Chinese Herbal medicine, as well as support the screening of natural phytophenols and their synthetic derivatives as effective antioxidants for cell transplantation purposes.

Methods

Plant and animals

Caoshanhu (LOT. 150210311) was purchased from Kangmei Pharmaceutical Co. Ltd (Shantou, China) and authenticated by Professor Shuhui Tan. Sprague–Dawley (SD) rats of 4 weeks of age were obtained from the Animal Center of Guangzhou University of Chinese Medicine.

Chemicals

Rosmarinic acid (CAS 20283-92-5, 98 %) was purchased from Shanghai Aladdin Chemistry Co., Ltd. (Shanghai, China); Astilbin (CAS 29838-67-3, 98 %) was from Chengdu Biopurify Phytochemicals Ltd. (Chengdu, China). Dulbecco's modified Eagle's medium (DMEM) and fetal bovine serum (FBS) were purchased from Gibco, Inc. (Grand Island, NY, USA). CD44 was from Wuhan Boster Co., Ltd. (Wuhan, China). DPPH• (1,1-diphenyl-2-picryl-hydrazl), neocuproine (2,9-dimethyl-1,10-phenanthroline), BHA (butylated hydroxyanisole), Trolox [(±)-6-hydroxyl-2,5,7,8-tetramethlychromane-2-carboxylic acid], Ferrozin [3-(2-pyridyl)-5,6-bis(4-phenylsulfonicacid)-1,2,4-triazine], Percoll system, and pyrogallol were obtained from Sigma-Aldrich Trading Co. (Shanghai, China); ABTS [2,2′-azino-bis(3-ethylbenzo-thiazoline-6-sulfonic acid diammonium salt)] and D-2-deoxyribose were from Amresco Chemical

Co. (Solon, OH, USA); DNA sodium salt (fish sperm) was purchased from Aladdin Chemistry Co. (Shanghai, China); Acetonitrile was purchased from Merck Serono Co., Ltd. (Shanghai, China); Acetonitrile and water were of HPLC grade. All other reagents were of analytical grade.

Preparation of ethanol extract of *S. glabra* (ESG)

The preparation of ethanol extract of *S. glabra* was based on the method [15]. In brief, the dried *S. glabra* (Caoshanhu) was ground into coarse powder then extracted with refluxing method using 18-fold ethanol for 6 h. The extract was filtered using Büchner funnel and filter paper. The ethanol extract was concentrated to dryness under reduced pressure at 60 °C using a rotary evaporator. The dried extract was named ethanol extract of *S. glabra* (ESG) and stored at 4 °C for further analysis.

Determination of total phenolics

The total phenolics of the ESG were determined using a modified Folin-Ciocalteu colorimetric method [16, 17]. In brief, 0.1 mL ESG methanolic solution (1 mg/mL) was mixed with 0.5 mL Folin-Ciocalteu reagent (0.25 mol/L). The mixture was left standing for 3 min, followed by the addition of Na_2CO_3 aqueous solution (1.0 mL, 15 %, *w/v*). After standing at room temperature for 30 min, the mixture was centrifuged at 3500 *g*/min for 3 min. The absorbance of the supernatant was measured at 760 nm (Unico 2100, Shanghai, China). The determinations were performed in triplicate, and the calculations were based on a calibration curve obtained with quercetin, the linear regression equation was $y = 0.1296x + 0.0848$ (x for quercetin content, y for absorbance at 760 nm, $R = 0.998$). The result was expressed as quercetin equivalents in milligrams per gram of extract.

HPLC analysis for RA and AS in ESG

HPLC analysis was performed on Waters e2695 (Los Angeles, California, USA) equipped with Agilent 5 TC-C_{18} (250 mm × 4.6 mm, 5 μm) (Beijing, China). The mobile phase consisted of acetonitrile (A)-0.5 % trifluoroacetic acid in water (B) (0~10 min, remain 15 % A; 10~50 min, 15 % A~25 % A; 50~80 min, 25 % A~80 % A; 80~85 min, 80 % A~15 % A), the flow rate was 1.0 mL/min, injection volume was 20 μL and absorption was measured at 254 nm [18]. In the study, RA and AS in ESG were identified by comparing their retention times and the peak areas were employed to characterize the relative contents of RA and AS using the linear regression equations $y = 1480.4x + 406{,}988$ ($R = 0.988$) and $y = 22753x + 462{,}876$ ($R = 0.962$), respectively.

Protecting MSCs against oxidative stressed apoptosis (MTT assay)

The MSCs were cultured according to a slightly modified version of the methods described in our previous report [19]. Briefly, bone marrow samples were obtained from the femurs and tibias of rats, and the resulting samples were diluted with DMEM (LG: low glucose) containing 10 % FBS. The MSCs were obtained by gradient centrifugation at 900 *g*/min for 30 min on a 1.073 g/mL Percoll system. The cells were then detached by treatment with 0.25 % trypsin and passaged into culture flasks at a density of 1×10^4 cells/cm^2. The homogeneity of the MSCs was evaluated at passage 3 based on their CD44 expression by flow cytometry. These cells were then used for the following experiments.

These MSCs were seeded into 96-well plates (4×10^3 cells/well). After adherence for 24 h, the cells were divided into three groups, including control, model and samples groups. The MSCs in the control group were incubated for 24 h in DMEM. The MSCs in the model group were injured for 1 h using $FeCl_2$ (100 μM) followed by H_2O_2 (50 μM). The resulting mixture of $FeCl_2$ and H_2O_2 was removed and the MSCs were incubated for 24 h in DMEM. The MSCs in the samples groups were injured and incubated for 24 h in DMEM in the presence of various concentrations of samples. After being incubated, the cells were treated with 20 μL of MTT (5 mg/mL in PBS), and the resulting mixtures were incubated for 4 h. The culture medium was subsequently discarded and replaced with 150 μL of DMSO. The absorbance of each well was then measured at 490 nm using a Bio-Kinetics plate reader (PE-1420; Bio-Kinetics Corporation, Sioux Center, IA, USA). The serum medium was used for the control group and each sample test was repeated in five independent wells.

Mechanistic chemistry experiments

Mechanistic chemistry experiments mainly included various antioxidant assays, e.g. DNA protection assay, •OH scavenging (deoxyribose degradation) assay, $\bullet O_2^-$ scavenging (pyrogallol autoxidation) assay, $ABTS^{+}\bullet$ scavenging assay, DPPH• scavenging assay, and Fe^{2+}-chelating assay. Among them, the former three methods have been established by our team [20–22]. The latter three methods were described in our previous paper [23]. In addition, FRAP (ferric ion reducing antioxidant power) assay was also performed in pH 3.6 buffer [24]. On the basis of the relevant formulas, the dose response curves were plotted to calculate IC_{50} values (in μg/mL). The IC_{50} values were then transferred into ones in molar unit (μM, Table 1). The detailed experimental protocols are shown in the additional file (Additional file 1).

Table 1 The IC_{50} values of ESG, rosmarinic acid (RA), astilbin (AS), and the positive controls

Assays	ESG μg/mL	RA μg/mL (μM)	AS μg/mL (μM)	Positive controls	
				Trolox μg/mL (μM)	BHA μg/mL (μM)
DNA protective effect	79.9 ± 10.4	44.9 ± 8.9 (126.7 ± 23.1[b])	70.9 ± 1.6 (193.3 ± 5.8[c])	85.0 ± 21.3 (85.0 ± 21.3[a])	67.8 ± 12.4 (376.3 ± 69.2[d])
•OH scavenging	109.5 ± 4.5	100.7 ± 0.9 (280.0 ± 1.0[b])	97.9 ± 5.5 (220.0 ± 10.0[a])	110.0 ± 4.6 (441.0 ± 20.1[d])	63.3 ± 7.8 (353.3 ± 41.6[c])
$\cdot O_2^-$ scavenging	140.8 ± 3.1	18.4 ± 0.4 (50 ± 0.4[a])	132.8 ± 3.4[b] (295.0 ± 7.5[b])	167.3 ± 11.1 (668.3 ± 40.2[c])	146.6 ± 4.4 (813.0 ± 24.0[d])
FRAP	24.9 ± 1.0	7.1 ± 1.2 (19.6 ± 3.2[b])	5.4 ± 0.2 (12.0 ± 0.4[a])	6.9 ± 0.3 (27.6 ± 1.2[c])	4.4 ± 0.2 (24.0 ± 1.1[c])
$ABTS^{+}\cdot$ scavenging	12.1 ± 1.8	6.8 ± 0.4 (18.7 ± 2.1[b])	5.0 ± 0.7 (11.1 ± 1.7[a])	7.2 ± 0.1 (29.0 ± 0.1[c])	5.9 ± 0.1 (33.3 ± 0.1[c])
DPPH• scavenging	48.6 ± 0.3	1.3 ± 0.1 (4.0 ± 0.1[a])	8.7 ± 0.2 (19.7 ± 5.8[d])	1.5 ± 0.1 (6.2 ± 0.1[b])	1.9 ± 0.1 (10.8 ± 0.3[c])
Fe^{2+} chelating	134.2 ± 15.6	128.1 ± 10.4 (355.7 ± 29.1[b])	218.8 ± 11.0 (485.0 ± 21.2[c])	63.9 ± 4.4 (217.3 ± 15.3[a])[d]	ND

IC_{50} value is defined as the concentration of 50 % effect percentage and expressed as mean ± SD ($n = 3$). Means values with different superscripts (a, b) in the same row are significantly different ($p < 0.05$), while with same superscripts are not significantly different ($p < 0.05$). [d]The positive control is sodium citrate.
BHA butylated hydroxyanisole, *ESG* Ethanolic extract of *Sarcandra glabra (Thunb.) Nakai*, *ND* Cannot be detected, *FRAP* ferric ion reducing antioxidant power

Statistical analysis

The IC_{50} values were calculated by linear regression analysis. All linear regression in this paper was analyzed by Origin 6.0 professional software. Determination of significant differences between the mean IC_{50} values of the sample and positive controls was performed using one-way ANOVA the *T*-test. The analysis was performed using SPSS software 13.0 (SPSS Inc., Chicago, IL) for windows. $P < 0.05$ was considered to be statistically significant.

Results and discussion

In the study, we first determined the total phenolics content of ESG using Folin-Ciocalteu reagent. The data suggested a high level of total phenolics (46.31 ± 0.56 mg quercetin/g) in ESG. The total phenolics mainly include caffeoyl derivatives and flavonoids, as mentioned above. In our study, a typical caffeoyl derivative RA and a flavonoid AS were successfully detected in ESG using HPLC (Fig. 2). The contents of RA and AS were 0.78 ± 0.01 % and 3.37 ± 0.01 %, respectively. In subsequent experiments, ESG along with RA and AS were investigated for their beneficial effect on oxidative-stressed MSCs.

As mentioned above, iron overload can cause oxidative stress-induced apoptosis [5], because it can yield •OH radicals through Fenton reaction (Eq. 1). Therefore, we used Fenton reagent (i.e. $FeCl_2$ *plus* H_2O_2) as the •OH radical generator for the study. As illustrated in Fig. 3a, ESG at 10–100 μg/mL could efficiently increase the viability of MSCs treated by Fenton reagent. This implies that ESG could protect MSCs from oxidative stress-induced apoptosis. Under the same concentrations,

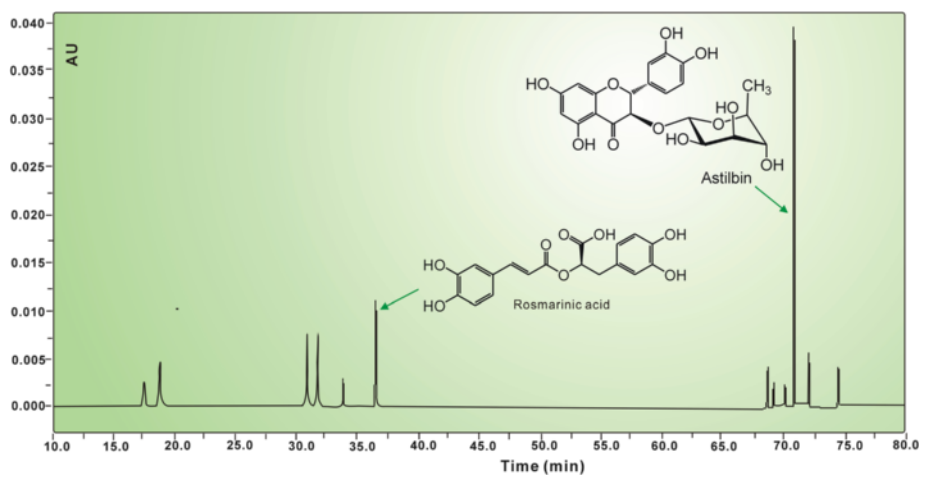

Fig. 2 A typical HPLC profile of ESG (ethanol extract of *Sarcandra glabra*)

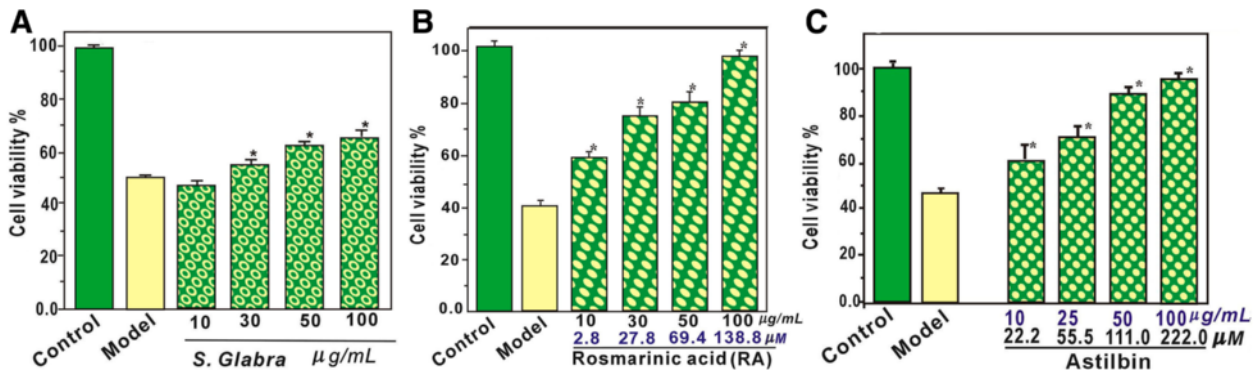

Fig. 3 Ethanolic extract of *Sarcandra glabra* (ESG, **a**), rosmarinic acid (RA, **b**), and astilbin (AS, **c**) prevent MSCs against Fenton-induced apoptosis. Cell viability was assessed using the MTT method. Experiments were performed with 3 different batches of cells and each batch was tested in triplicate. Data are the mean ± SD values. (*) $p < 0.05$, compared with MSCs damage following $FeCl_2$ *plus* H_2O_2

interestingly, RA and AS exhibited a better protective effect than ESG (Fig. 3). The findings might partially explain the beneficial effects of Caoshanhu on various diseases related to *heat-toxic* in TCM and support the rationality of RA and AS as two typical bioactive compounds. More importantly, these observations also suggest RA and AS as two good candidates for transplantation therapy based on MSCs.

$$Fe^{2+} + H_2O_2 \rightarrow Fe^{3+} + \bullet OH + OH^- \quad (1)$$

Oxidative-stressed apoptosis is suggested to closely associate with •OH-induced DNA oxidative lesions (e.g. 8-hydroxy-2′-deoxyguanosine and 8-oxo-7, 8-dihydroguanine) [25, 26]. Accordingly, we assayed its protection on DNA using a previously described approach [20]. As seen in Fig. 4a, ESG, RA, and AS (at 20–110 μg/mL) effectively prevented •OH-mediated DNA damage. This is consistent with the previous report that ESG, RA and AS played crucial roles in anti-cancer [27, 28], because carcinogenesis has been demonstrated to arise from oxidative stress. Similar results can also be observed in the •OH radical-scavenging assay based on deoxyribose degradation (Fig. 4b), where ESG, RA, and AS increased their •OH radical-scavenging activities in a concentration-dependent fashion. The similarity of the dose response curves between Fig. 4a and b indicated that their protection on MSCs and DNA were mainly based on ROS scavenging (especially •OH radical-scavenging). ESG, RA, and AS

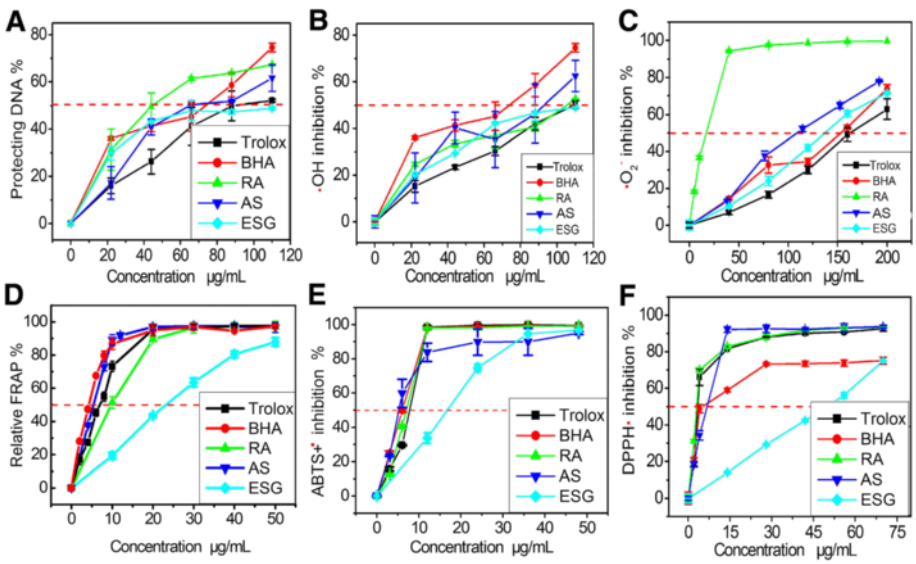

Fig. 4 The dose response curves of ESG, rosmarinic acid (RA), and astilbin (AS) in a series of antioxidant assays: (**a**) protective effect against DNA damage; (**b**) hydroxyl (•OH) radical-scavenging; (**c**) superoxide anion ($\bullet O_2^-$) radical-scavenging assay; (**d**) FRAP (ferric ion reducing antioxidant power); (**e**) $ABTS^{\bullet+}$ radical-scavenging assay; and (**f**) DPPH radical-scavenging assay. Each value is expressed as mean ± SD ($n = 3$); *ESG* ethanol extract of *Sarcandra glabra*, Trolox and BHA (butylated hydroxyanisole) were used as the positive controls

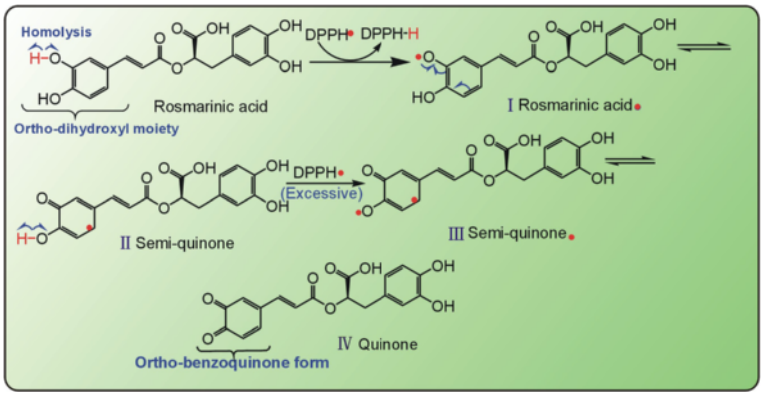

Fig. 5 The possible reaction of rosmarinic acid (RA) with DPPH• via hydrogen atom transfer (HAT) pathway

exhibited slight differences (Fig. 4a and b) because the •OH radical with its extreme reactivity can damage all types of chemical structures.

However, in the $\bullet O_2^-$ radical scavenging assay, we observed a significant ($p < 0.05$) difference among ESG, RA, and AS (Fig. 4c). As shown in Table 1, their relative $\bullet O_2^-$-scavenging levels decreased in the order of RA>AS>ESG. This order can better reflect the relative ROS-scavenging levels among the three samples, because $\bullet O_2^-$ radical is a milder and typical form of ROS. However, it is worth mentioning that, the previous data about the $\bullet O_2^-$-scavenging of AS were incorrect, because the researchers used alkaline buffer (e.g. pH 10 [29], pH 8.0 [30]) for the investigation. Under such alkaline condition, ionization of phenolic –OH as acid would predominate the chemical action to generate H^+ and PhO^-. PhO^-, however, underwent electron-donating inductive effect (+I) to enhance the next O-H bond in phenolic –OH to lessen the possibility of its homolysis, then to reduce the radical-scavenging level [21, 31]. Thus, abnormal dose response curves were observed in the previous study, in which the $\bullet O_2^-$-scavenging level of AS was even lower than that of a plant extract containing AS [30].

The difference of the three samples in $\bullet O_2^-$ scavenging level is assumed to be linked to the antioxidant mechanisms and their chemical structures. In the aspect of mechanistic chemistry, both $\bullet O_2^-$ scavenging and •OH scavenging are considered to be mediated through electron transfer (ET) and hydrogen atom transfer (HAT, or hydrogen-donating) [31–34].

To examine the possibility of ET, we analyzed ESG, RA, and AS by FRAP. The data suggested that they can reduce Fe^{3+} to Fe^{2+} with high efficiency (Fig. 4d). This assay was conducted under acidic condition wherein the ionization of H^+ was thus suppressed by environment and only ET can take place [35]. Our data in Fig. 4d and Table 1 clearly suggest the possibility of ET.

However, the IC_{50} values in FRAP assay revealed that AS was higher than RA (Table 1), regardless whether these compounds similarly contain four phenolic –OH groups. This may be because compared with RA, AS has a larger planar conjugation system (i.e. A/C fused rings) to delocalize the positive charges after ET [36]. Our assumption is further supported by the results from the ABTS•$^+$ assay, in which AS displayed lower IC_{50} value than RS (Table 1) and a similar trend of dose response

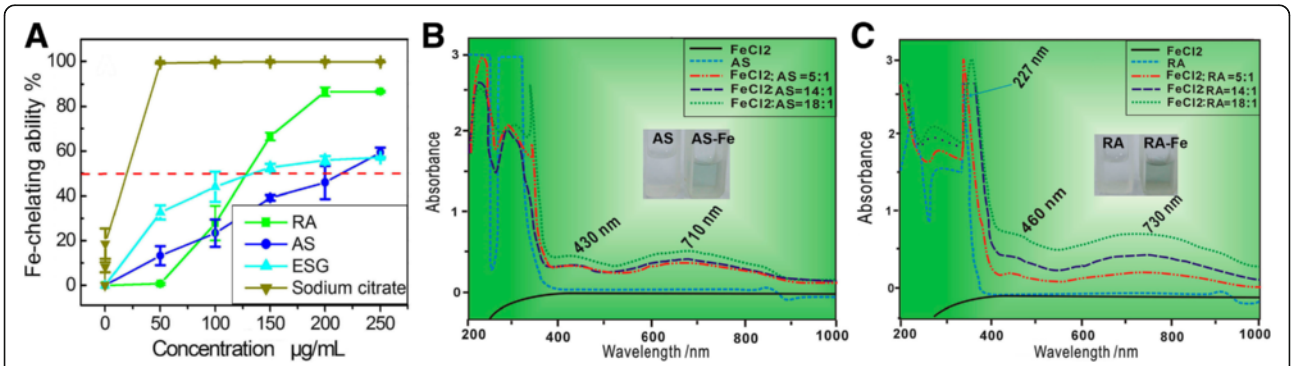

Fig. 6 The dose response curve of rosmarinic acid (RA), astilbin (AS) in the Fe^{2+}-chelating assay (**a**), the UV spectra of AS-Fe^{2+} complex (**b**), RA-Fe^{2+} complex (**c**). In figure a, each value is expressed as Mean ± SD ($n = 3$). Sodium citrate was used as positive control

curve to that in FRAP assay (Fig. 4e). ABTS•$^{+}$ scavenging, however, was interrupted to comprise a partially reversible ET mechanism [37].

To test the possibility of HAT, we further explored the DPPH•-scavenging capacities of the compounds. As illustrated in Fig. 4f, AS presented a good DPPH•-scavenging activity. The DPPH•-scavenging activity is reported to be affected by various factors, such as pH [38], solvent [39, 40], steric hindering [41], H-bonding [42], and mediated by several types of mechanisms, such as HAT [43], sequential electron proton transfer (SEPT) [43], ET [35], radical adduct formation (RAF) [43], sequential proton loss electron transfer (SPLET) [40], and proton-coupled electron transfer (PCET) [44]). Nevertheless, HAT is regarded as an essential mechanism [43, 45]. Accordingly, DPPH is usually used to evaluate the HAT potential of an antioxidant [46]. The fact that ESG, along with RA and AS, can scavenge DPPH•, suggested that HAT possibly happened to account for the antioxidant activity. However, in this aspect, AS had weaker HAT potential than RA, although both of them contain four phenolic –OH groups (Fig. 2).

The difference can be attributed to their chemical structures. With the AS molecule, a steric hindrance from the residue of 3-α-L-rhamnose can limit the atom transfer from antioxidant molecule to radical, and H-bonding between 5–OH and 4–C = O may decrease the homolysis of phenolic –OH [41, 42]. However, the above disadvantageous factors for HAT do not occur with the RA molecule. Conversely, the RA molecule bears two moieties with HAT potential. As such, RA can easily undergo HAT pathways to transfer into stable *ortho*-quinone form (Fig. 5).

As stated in the Methods section, the generation of DPPH• and ABTS•$^{+}$ do not rely on metal catalysis, and therefore, their DPPH• and ABTS•$^{+}$ radical scavenging capacities may be mediated through direct radical-scavenging. On the contrary, the generation of ROS (especially •OH) radical relies on transition metal catalysis (Eq. 1). Hence, Fe^{2+}-chelation can decrease the level of •OH radicals and is regarded as indirect •OH radical scavenging [47]. The present study used Ferrozine as the indicator to investigate Fe-chelating abilities. As seen in Fig. 6, ESG, RA, and AS increased Fe^{2+}-chelating percentages at 50–250 μg/mL in a concentration-dependent manner. This provides the evidence of Fe^{2+}-chelating as an indirect approach for phytophenols to scavenge •OH radicals and then to relieve oxidative stress in MSCs. This is consistent with the result of animal experiment that caffeic acid with catechol moiety could inhibit oxidative stress mediated by iron overload in rats [48]. In fact, some iron chelators (e.g. deferiprone) were reported to be able to completely inhibit the generation of •OH radicals [49].

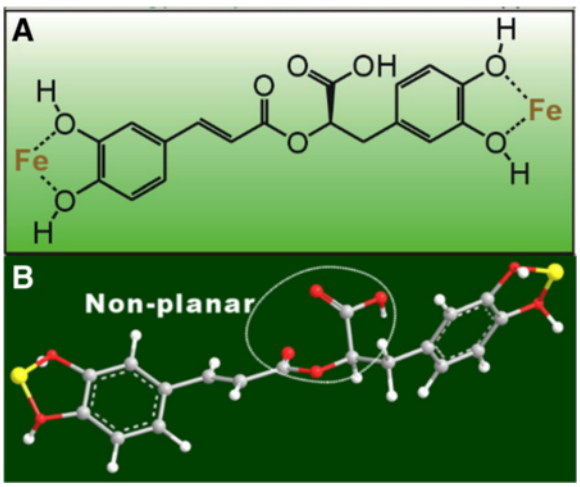

Fig. 7 The proposed structure of rosmarinic acid (RA) chelated with Fe^{2+} (**a**), and the ball-stick model of rosmarinic acid (RA, **b**)

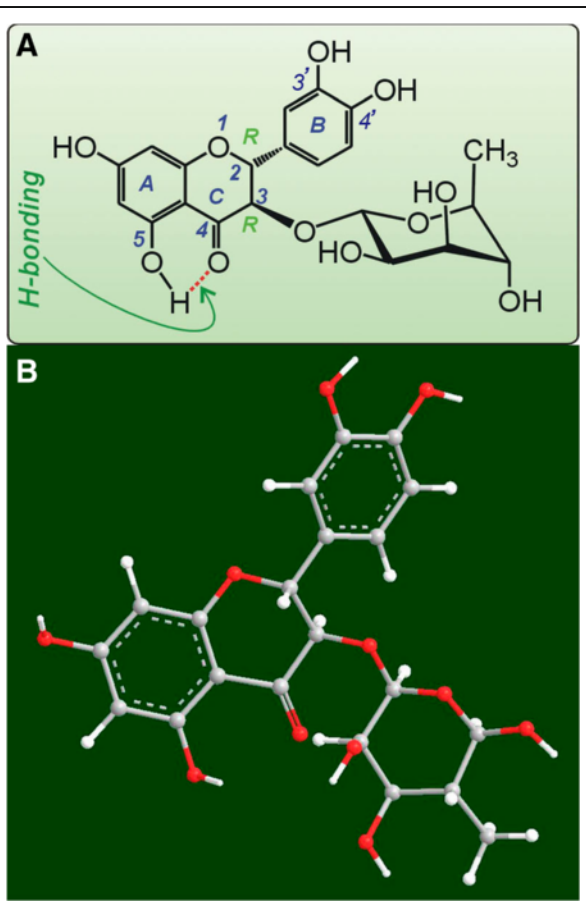

Fig. 8 The H-bonding (**a**), and ball-stick model of astilbin (AS) based on preferential conformation (**b**)

However, in the case of iron overload, these phenolics could also reduce Fe^{3+} to Fe^{2+}, and recycling of Fe^{2+} source that could cause the formation of •OH radicals (Eq. 2). Our results agree with the previous studies that iron reduction potentiates •OH radical formation in flavonols with catechol moiety [50]. The recycling described in Eq. 2 can also explain the metal-dependent pro-oxidant action of gallic acid derivatives or (−)-epigallocatechin-3-gallate (EGCG), which can cause cell apoptosis and formation of 8-hydroxy-2′-deoxyguanosine [51, 52].

$$H_2O_2 + Fe^{2+} \xrightarrow{\text{Phytophenol}} Fe^{3+} + \cdot OH + OH^- \quad (2)$$

Thereby, under the iron overload and aerobic condition, administration of massive flavonoids may lead to unpredictable consequences [50]. The safest approach may be administration of some iron chelators without reducing power such as deferiprone or deferoxamine [53].

In our experiment of Fe^{2+}-chelating, we observed a great difference between RA and AS. The colorless RA solution was found to turn green when mixed with $FeCl_2$ (Fig. 6b). The RA-Fe^{2+} complex presented an absorption maximum at 730 nm, while RA itself showed an absorption maximum at 227 nm. The great bathochromic shift (λ_{max} 227 → 730 nm) evidently indicates an extension of aromatic conjugation. The metal-chelating has been reported to come from *ortho*- or adjacent –OH and –C = O groups [43]. A possible structure of the RA-Fe^{2+} complex is shown in Fig. 7a. It is noted that, the adjacent –C = O and –COOH groups cannot chelate Fe^{2+}, since two groups are non-planar and cannot form a stable ring with Fe^{2+} (Fig. 7b). Compared with RA, AS exhibited lower Fe^{2+}-chelating percentages (Fig. 6a). The strength of the absorption maximum of AS-Fe^{2+} complex also became weaker (Fig. 6b and c), while AS-Fe^{2+} complex appeared a bit less green as compared to RA-Fe^{2+} complex (Fig. 6b and c). Quantitative analysis based on IC_{50} values further suggested that the Fe^{2+}-chelating level of AS was only 0.72 (355/485) times than that of RA (Table 1).

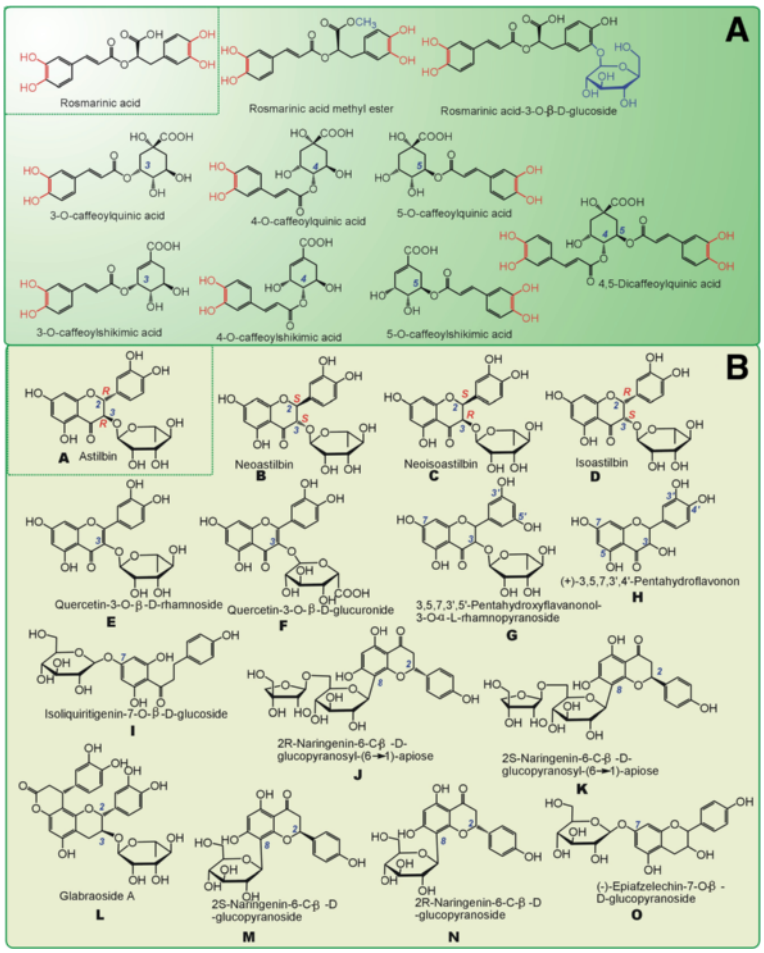

Fig. 9 The structures of caffeoyl derivatives (**a**) and flavonoids (**b**) in *S. glabra* [12] (The structure of L glabraoside A is corrected based on [51])

Such difference might also be attributed to the chemical structure. Seemingly, in AS molecule, there are two chelating sites, i.e. 3′, 4′-dihydroxy groups (catechol moiety), and between 4–C = O and 5–OH groups (Fig. 8a). However, the H-bonding between 4–C = O and 5–OH groups may hinder the form of Fe^{2+}-chelating. Moreover, the steric hindrance from the residue of α-L-rhamnose in 3-position can also reduce the possibility of Fe^{2+}-chelating at this site (Fig. 8b).

It must be emphasized that, the antioxidant features of RA can be generalized to other caffeoyl derivatives in ESG, because all of these derivatives similarly bear the caffeoyl moieties (Fig. 9a); while those of AS cannot be generalized to other flavonoids because of the difference in chemical structures, such as diflavonone glycosides (A-D, G, J, K, M, N, O), flavonone glycosides (E & F), flavonol (H), chalcone (I), and even flavan lactone (L) (Fig. 9b) [12, 54].

Conclusion

The traditional Chinese Herb medicine *S. glabra* can protect MSCs from oxidative-stressed apoptosis. Such protective effect can be attributed to its antioxidant ability and to the presence of two kinds of phytophenols, caffeoyl derivatives and flavonoids. As the respective representatives of caffeoyl derivatives and flavonoids, rosmarinic acid and astilbin may exert the antioxidant action via direct ROS-scavenging, and indirect ROS-scavenging (i.e. Fe^{2+}-chelating). The direct ROS-scavenging may involve hydrogen atom transfer (HAT) and/or electron transfer (ET) pathways. Astilbin possibly engages the latter pathway due to the larger planar conjugation in A/C fused rings. Rosmarinic acid, on the other hand, presents more HAT and Fe^{2+}-chelating ability which can be attributed to rosmarinic acid bearing one more catechol moiety. Astilbin has steric-hindrance from 3-α-L-rhamnose and an H-bonding between 4,5 sites. The antioxidant features of rosmarinic acid can be generalized to other caffeoyl derivatives, while that of astilbin cannot be generalized to other flavonoids because of the difference in chemical structures.

Additional file

Additional file 1: Experimental protocols for mechanistic chemistry. (DOCX 24 kb)

Abbreviations

ABTS: [2,2′-azino-bis(3-ethylbenzo-thiazoline-6-sulfonic acid diammonium salt)]; AS: Astilbin; BHA: Butylated hydroxyanisole; DMEM: Dulbecco's modified Eagle's medium; DPPH•: (1,1-diphenyl-2-picryl-hydrazl); ESG: Ethanol extract of *Sarcandra glabra*; ET: Electron transfer; FBS: Fetal bovine serum; HAT: Hydrogen atom transfer; MSCs: Mesenchymal stem cells; MTT: [3-(4,5-dimethylthiazol-2-yl)-2,5-diphenyl]; RA: Rosmarinic acid; ROS: Reactive oxygen species; *S. glabra*: *Sarcandra glabra* (Thunb.) Nakai; SD: Standard deviation; TBA: 2-thiobarbituric acid; TCM: Tradition Chinese Medicine; Tris: Tri-hydroxymethylamino methane; Trolox: [(±)-6-hydroxyl-2,5,7,8-tetramethylchromane-2-carboxylic acid]

Acknowledgements

None.

Funding

This work was supported by the National Nature Science Foundation of China (81273896, 81573558), and High Level Universities Construction Special Foundation of Guangdong in 2015 (2050205), Guangdong Science and Technology Project (2016A050503039).

Availability of data and materials

Data are all contained within the article.

Authors' contributions

XCL and CDF conceived and designed the experiments; JJL and JL performed the experiments; QJ conducted the TPTZ assay; TTW and YQL analyzed the data; XCL wrote the paper. All authors read and approved the final manuscript.

Competing interests

The authors declare that they have no competing interests.

Consent for publication

Not applicable.

Ethics approval and consent to participate

The Institution Animal Ethics Committee in Guangzhou University of Chinese Medicine (Guangzhou, China) approved the protocols used in this study.

Received: 3 June 2016 Accepted: 4 October 2016
Published online: 28 October 2016

References

1. Rosenbaum AJ, Grande DA, Dines JS. The use of mesenchymal stem cells in tissue engineering: a global assessment. Organogenesis. 2008;4:23–7.
2. Torrente Y, Polli E. Mesenchymal stem cell transplantation for neurodegenerative diseases. Cell Transplant. 2008;17:1103–13.
3. Mamidi MK, Das AK, Zakaria Z, Bhonde R. Mesenchymal stromal cells for cartilage repair in osteoarthritis. Osteoarthritis Cartilage. 2016;10:1016.
4. Luo F, Liu T, Wang J, Li J, Ma P, Ding H, Feng G, Lin D, Xu Y, Yang K. Bone marrow mesenchymal stem cells participate in prostate carcinogenesis and promote growth of prostate cancer by cell fusion in vivo. Oncotarget. 2016;10:18632.
5. Nicolay NH, Lopez PR, Saffrich R, Huber PE. Radio-resistant mesenchymal stem cells: mechanisms of resistance and potential implications for the clinic. Oncotarget. 2015;6:19366–80.
6. Zhang Y, Zhai W, Zhao M, Li D, Chai X, Cao X, Meng J, Chen J, Xiao X, Li Q, Mu J, Shen J, Meng A. Effects of iron overload on the bone marrow microenvironment in mice. PLoS One. 2015;10:e0120219.
7. Sung KW, Lim DH, Yi ES, Choi YB, Lee JW, Yoo KH, Koo HH, Kim JH, Suh YL, Joung YS, Shin HJ. Tandem high-dose chemotherapy and autologous stem cell transplantation for atypical teratoid/rhabdoid tumor. Cancer Res Treat. 2016. doi:10.4143/crt.2015.347.
8. Wang HH, Cui YL, Zaorsky NG, Lan J, Deng L, Zeng XL, Wu ZQ, Tao Z, Guo WH, Wang QX, Zhao LJ, Yuan ZY, Lu Y, Wang P, Meng MB. Mesenchymal stem cells generate pericytes to promote tumor recurrence via vasculogenesis after stereotactic body radiation therapy. Cancer Lett. 2016;375:349–59.
9. Yang SR, Park JR, Kang KS. Reactive oxygen species in mesenchymal stem cell aging: implication to lung diseases. Oxid Med Cell Longev. 2015;10:486263.
10. China Pharmacopoeia Committee. Pharmacopoeia of the People's Republic of China. Beijing: China Press of Traditional Chinese Medicine; 2015.
11. Fang YZ, Zheng RL. Theory and application of free radical biology. 2nd ed. Beijing: Science Press; 2002.
12. Li X, Zhang YF, Zeng X, Yang L, Deng YH. Chemical profiling of bioactive constituents in *Sarcandra glabra* and its preparations using ultra-high-pressure liquid chromatography coupled with LTQ Orbitrap mass spectrometry. Rapid Commun Mass Sp. 2011;25:2439–47.
13. Deng SS, Ma HX, Liu ZJ, Xu RQ, Hu MF. Content determination of isofraxidin, rosmarinic acid and astilbin from Herba Sarcandrae in different artificial cultivate. J Pharm Prac. 2011;29:2000–3.

14. Lin PL. Quality evaluation and relevant pharmacodynamics of *sarcandra glabra*. M pharm thesis. China: Fujian University of Chinese Medicine; 2013.
15. Abbasi Oshaghi E, Khodadadi I, Saidijam M, Yadegarazari R, Shabab N, Tavilani H, et al. Lipid lowering effects of hydroalcoholic extract of Anethum graveolens L. and dill tablet in high cholesterol fed hamsters. Cholesterol. 2015;2015:958560.
16. Li X, Lin J, Han L, Mai W, Wang L, et al. Antioxidant ability and mechanism of rhizoma Atractylodes macrocephala. Molecules. 2012;17:13457–72.
17. Oshaghi A, Tavilani H, Khodadadi I, Goodarzi MT. Dill tablet: a potential antioxidant and anti-diabetic medicine. Asian Pacific Journal of Tropical Biomedicine. 2015;5:720–7.
18. Zhao RZ, Zhao Y, Zhang LQ, Lu CJ. Determination of isofraxidin and astilbin by HPLC in rat plasma and its application after orally administration the extract of Sarcandra glabra. Pak J Pharm Sci. 2013;26:1–6.
19. Li X, Han L, Li Y, Zhang J, Chen J, Lu W, Zhao X, Lai Y, Chen D, Wei G. Protective effect of sinapine against hydroxyl radical-induced damage to mesenchymal stem cells and possible mechanisms. Chem Pharm Bull (Tokyo). 2016;64:319–25.
20. Li X, Mai WQ, Wang L, Han WJ. A hydroxyl-scavenging assay based on DNA damage in vitro. Anal Biochem. 2013;438:29–31.
21. Li X. Solvent effects and improvements in the deoxyribose degradation assay for hydroxyl radical-scavenging. Food Chem. 2013;141:2083–8.
22. Li X. Improved pyrogallol autoxidation method: a reliable and cheap superoxide-scavenging assay suitable for all antioxidants. J Agri Food Chem. 2012;60:6418–24.
23. Li X, Lin J, Gao YX, Han WJ, Chen DF. Antioxidant activity and mechanism of Rhizoma Cimicifugae. J Chem Cent. 2012;6:140–50.
24. Benzie IF, Strain JJ. The ferric reducing ability of plasma (FRAP) as a measure of "antioxidant power": the FRAP assay. Anal Biochem. 1996;239:70–6.
25. Lin J, Li X, Chen L, Lu WZ, Chen XW, Han L, Chen DF. Protective effect against hydroxyl radical-induced DNA damage and antioxidant mechanism of [6]-gingerol: a chemical study. Bull Korean Chem Soc. 2014;35:1633–8.
26. Myoren T, Kobayashi S, Oda S, Nanno T, Ishiguchi H, Murakami W, Okuda S, Okada M, Takemura G, Suga K, Matsuzaki M, Yano M. An oxidative stress biomarker, urinary 8-hydroxy-2′-deoxyguanosine, predicts cardiovascular-related death after steroid therapy for patients with active cardiac sarcoidosis. Int J Cardio. 2016;212:206–13.
27. Wu CF, Karioti A, Rohr D, Bilia AR, Efferth T. Production of rosmarinic acid and salvianolic acid B from callus culture of Salvia miltiorrhiza with cytotoxicity towards acute lymphoblastic leukemia cells. Food Chem. 2016;201:292–7.
28. Elansary HO, Mahmoud EA. In vitro antioxidant and antiproliferative activities of six international basil cultivars. Nat Prod Res. 2015;29:2149–54.
29. Haraguchi H, Mochida Y, Sakai S, Masuda H, et al. Protection against oxidative damage by dihydroflavonols in engelhardtia chrysolepis. Biosci Biotechnol Biochem. 1996;60:945–8.
30. Zhang QF, Zhang ZR, Cheung HY. Antioxidant activity of Rhizoma Smilacis Glabrae extracts and its key constituent-astilbin. Food Chem. 2009;115:297–303.
31. Jovanovic SV, Steenken S, Simic MG, Hara Y. Antioxidant potential of gallocatechins-a pulse radiolysis and laser photolysis study. J Am Chem Soc. 1995;117:9881–8.
32. Bergeron F, Auvré F, Radicella JP, Ravanat JL. HO• radicals induce an unexpected high proportion of tandem base lesions refractory to repair by DNA glycosylases. PNAS. 2010;107:5528–33.
33. Taicheng A. Kinetics and mechanism of •OH mediated degradation of dimethyl phthalate in aqueous solution: experimental and theoretical studies. Environ Sci Technol. 2014;48:641–8.
34. Li DD. Hydroxyl radical reaction with trans-resveratrol: initial carbon radical adduct formation followed by rearrangement to phenoxyl radical. J Phys Chem B. 2012;116:7154–61.
35. Gülçin İ. Antioxidant activity of food constituents: an overview. Arch Toxicol. 2012;86:345–91.
36. Monica L, Tiziana M, Nino R, Marirosa T. Antioxidant properties of phenolic compounds: H-atom versus electron transfer mechanism. J Phys Chem A. 2004;108:4916–22.
37. Aliaga C, Lissi EA. Reaction of 2, 2′-azinobis (3-ethylbenzothiazoline-6-sulfonic acid (ABTS) derived radicals with hydroperoxides Kinetics and mechanism. Int J Chem Kinet. 1998;30:565–70.
38. Xie J, Schaich KM. Re-evaluation of the 2, 2-Diphenyl-1-picrylhydrazyl free radical (DPPH) assay for antioxidant activity. J Agri Food Chem. 2014;62:4251–60.
39. Litwinienko G, Ingold KU. Abnormal solvent effects on hydrogen atom abstractions. 1. The reactions of phenols with 2, 2-diphenyl-1-picrylhydrazyl (dpph•) in alcohols. J Org Chem. 2003;68:3433.
40. Litwinienko G, Ingold KU. Abnormal solvent effects on hydrogen atom abstraction. 3. Novel kinetics in sequential proton loss electron transfer chemistry. J Org Chem. 2005;70:8982–90.
41. Wright JS, Johnson ER, DiLabio GA. Predicting the activity of phenolic antioxidants: theoretical method, analysis of substituent effects, and application to major families of antioxidants. J Am Chem Soc. 2001;123:1173–83.
42. Oyais AC, Muzaffar HN, Mohammad AM, Ghulam MR, Aijaz AD. Effects of surfactant micelles on solubilization and DPPH radical scavenging activity of Rutin. J Colloid Interf Sci. 2011;355:140–9.
43. Li X, Gao YX, Li F, Liang A, Xu Z, Bai Y, et al. Maclurin protects against hydroxyl radical-induced damages to mesenchymal stem cells: Antioxidant evaluation and mechanistic insight. Chem Biol Interact. 2014;219:221–8.
44. Maria AA, Mario B, Nicola C, Francesca C, Patrizia D, Marco F, Guido F, Barbara G, Angela LB, Osvaldo L, et al. DPPH radical scavenging activity of paracetamol analogues. Tetrahedron. 2012;68:10180–7.
45. Wang LF, Zhang HY. A theoretical investigation on DPPH radical-scavenging mechanism of edaravone. Bioorg Med Chem Lett. 2003;13:3789–92.
46. Ariane B, Juliana T, Grzegorz B, Safae EH, Rachid B, Anne SM, Pierre L. High-performance liquid chromatographic method to evaluate the hydrogen atom transfer during reaction between 1, 1-diphenyl-2-picryl-hydrazyl radical and antioxidants. Anal Chim Acta. 2012;711:97–106.
47. Fang YZ, Zheng RL. Theory and application of free radical biology. vol 469. 1st ed. Beijing: Science Press; 2002. p. 98–9.
48. Lafay S, Gueux E, Rayssiguier Y, Mazur A, Rémésy C, Scalbert A. Caffeic acid inhibits oxidative Stress and reduces hypercholesterolemia induced by iron overload in rats. Int J Vitam Nutr Res. 2005;75:119–25.
49. Timoshnikov VA, Kobzeva TV, Polyakov NE, Kontoghiorghes GJ. Inhibition of Fe^{2+}- and Fe^{3+}- induced hydroxyl radical production by the iron-chelating drug deferiprone. Free Radic Biol Med. 2015;78:118–22.
50. Macáková K, Mladěnka P, Filipský T, Říha M, Jahodář L, Trejtnar F, Bovicelli P, Proietti Silvestri I, Hrdina R, Saso L. Iron reduction potentiates hydroxyl radical formation only in flavonols. Food Chem. 2012;135:2584–92.
51. Yoshino M, Haneda M, Naruse M, Htay HH, Iwata S, Tsubouchi R, Murakami K. Prooxidant action of gallic acid compounds: copper-dependent strand breaks and the formation of 8-hydroxy-2′-deoxyguanosine in DNA. Toxicol in Vitro. 2002;16:705–9.
52. Azam S, Hadi N, Khan NU, Hadi SM. Prooxidant property of green tea polyphenols epicatechin and epigallocatechin-3-gallate: implications for anticancer properties. Toxicol in Vitro. 2004;18:555–61.
53. Devos D, Moreau C, Devedjian JC, Kluza J, Petrault M, Laloux C, Jonneaux A, Ryckewaert G, Garçon G, Rouaix N, Duhamel A, Jissendi P, Dujardin K, Auger F, Ravasi L, Hopes L, Grolez G, Firdaus W, Sablonnière B, Strubi-Vuillaume I, Zahr N, Destée A, Corvol JC, Pöltl D, Leist M, Rose C, Defebvre L, Marchetti P, Cabantchik ZI, Bordet R. Targeting chelatable iron as a therapeutic modality in Parkinson's disease. Antioxid Redox Sign. 2014;21:195–210.
54. Takara K, Kuniyoshi A, Wada K, Kinjyo K, Iwasaki H. Antioxidative flavan-3-ol glycosides from stems of Rhizophora stylosa. Biosci Biotechnol Biochem. 2008;72:2191–4.